OBSERVED ENTRAINMENT IN A POWER PLANT PLUME

by

JOHN S. LAGUE

B.S., University of California, Davis
(1970)

SUBMITTED IN PARTIAL FULFILLMENT OF THE
REQUIREMENTS FOR THE DEGREE OF
MASTER OF SCIENCE

at the

MASSACHUSETTS INSTITUTE OF TECHNOLOGY
May, 1970 (i.e. June 1973)

Signature of Author.....
Department of Meteorology, May 11, 1973

Certified by.....
Thesis Supervisor

Accepted by.....
Chairman, Departmental Committee
on Graduate Students

ABSTRACT

OBSERVED ENTRAINMENT IN A POWER PLANT PLUME

by

JOHN S. LAGUE

Submitted to the Department of Meteorology on May 11, 1973
in partial fulfillment of the requirements for
the degree of Master of Science

Detailed measurements of plume cross sections are used to investigate the spread of effluent released from tall chimneys. The dependence of plume size and shape characteristics upon relevant meteorological parameters is investigated. In particular, the sensitivity of the entraining plume's configuration to variations of wind speed, directional wind shear, and atmospheric stability is discussed. Low wind speeds are found to be strongly associated with large vertical variations in wind direction, and with maximum plume rise. Thus light winds appear to mitigate in favor of large, diffuse plumes. This is contrary to the normal modelling assumption of an inverse proportionality between wind speed and downwind concentrations.

The ordinary approach in simulating the diffusion of buoyant emissions from an elevated source involves postulating a virtual point source at an "effective stack height" above the true source. All of the plume's growth is attributed to the action of ambient turbulence upon a passive effluent. The results obtained in this study indicate that such treatments lead to substantial underpredictions of downwind cross-sectional size with a neutral or stable vertical temperature profile. An argument is presented which attributes this observed discrepancy to the importance of the initial entrainment phase, where self-induced mixing, rather than ambient turbulence is the dominant mechanism. A technique is suggested whereby upwind virtual-source correction distances may be employed in the standard models to improve their predictive capabilities for elevated source applications.

Measurements of plume rise under stable and neutral conditions show, on the average, good agreement with predictions made with the formulae proposed by Briggs. The inherent and commonly-observed variability of the vertical temperature gradient through the lower layer of the atmosphere inevitably leads to a large scatter about this general agreement, since the plume-rise formulae ignore such variability.

An extrapolation of measured plume cross sections is undertaken to simulate the size-shape characteristics of plumes at the downwind distance corresponding to maximum rise. The value of the entrainment "constant" is seen to depend primarily upon the choice of a definition for the plume "edge".

Thesis Supervisor: James M. Austin, Professor of Meteorology.

ACKNOWLEDGEMENT

The author benefited greatly from the enthusiastic participation in this work by Professor James M. Austin. As thesis advisor, he provided many useful suggestions. A debt of gratitute is also owed to the management and personnel of Environmental Research and Technology, Lexington, Massachusetts, for freely extending the use of calculating equipment and for help in preparing tables and diagrams.

TABLE OF CONTENTS

LIST OF TABLES

LIST OF FIGURES

I. INTRODUCTION

There exist certain inconsistencies in present-day attempts to model the diffusion of effluents emitted several hundred meters above the ground. Industry, in an effort to diminish its contributions to ground-level pollutant concentrations, is resorting to the use of taller and taller stacks. The diffusion meteorologist is frequently called upon to provide estimates of the dispersion of material emitted from these elevated sources. In many respects, he has been ill-equipped to do so.

Most currently-employed models incorporate diffusion coefficients which are based upon empirical observations of the turbulent fluctuations of low-level winds, and the resulting statistics have been correlated with observations of plume spread to derive functional forms of horizontal and cross-wind diffusion parameters. One of the more widely used treatments, based upon the work of Pasquill[1], Cramer[2], and Gifford[3], is presented in Turner's Workbook of Atmospheric Dispersion Estimates[4]. Turner suggests that the spread parameters which appear in his model "...are most applicable to ground-level or low-level releases (from the surface to about 20 meters)". Yet lacking coordinated studies of wind fluctuations and plume characteristics at higher levels, most attempts to describe diffusion from tall stack sources appeal to these same coefficients with something of a cavalier, hope-for-the-best rationale.

A second area of uncertainty concerns the relative importance of the several mixing mechanisms which sequentially dominate the spread

of a plume subsequent to emission from large stacks. Initially, the process is one of a hot jet of turbulent gases introduced with considerable vertical velocity into a regime of predominantly horizontal flow. In view of the high temperatures and exit velocities typical of large power plant effluents, it must be of fundamental concern to determine the extent to which this phase of entrainment influences the ultimate properties of the plume cross sections downwind. The usual assumption is that the total growth of a plume is explainable in terms of a passive effluent acted upon by ambient turbulence. The plume is allowed to rise some distance above the physical top of the stack determined by a plume rise formula, but the downwind spread is commonly treated as atmospheric dispersion from a point source at an "effective stack height", with the origin above the stack. Especially for large source applications, it seems more likely that the rate of mixing with the environmental air in the first stage of plume rise is governed by the initial properties of the effluent itself, and by the specific environmental conditions of wind shear, wind speed, and atmospheric stability. This study addresses itself to determining the relative importance of these factors in the entrainment process.

Notable in recent literature on the subject of plume rise are the works of Briggs[5], and Slawson and Csanady[6]. Both treatments employ the entrainment hypothesis, first proposed by Taylor[7], to solve the differential equations for mass continuity, conservation of momentum, and conservation of buoyancy. The ultimate success of the resulting plume rise models hinges upon the assignment of proper values to the entrainment constants under specific atmospheric conditions.

Such a determination must come from observational data. A similar need for experimental documentation exists in order to determine whether the inherent variability of lapse rate, wind velocity in the vertical, etc., invalidate formulae based on models which ignore such variability.

The approach adopted in this investigation is, therefore, mainly an empirical one. An excellent basis for a study of the growth of plumes from very large stacks is provided by the U. S. Public Health Services' Large Power Plant Effluent Study (LAPPES). The unique value of the LAPPES data set is the detailed information it provides concerning the dimensional characteristics of plume cross sections, with corresponding meteorological measurements defining the vertical structure of the wind and temperature fields. As a result, it is felt that these data are particularly amenable to the pursuit of the following objectives:

(1) To evaluate the applicability of standard diffusion coefficients (such as Turner's σ_y and σ_z), for describing the growth of plumes from elevated sources.

(2) To determine the importance of relevant meteorological parameters insofar as they influence the size and shape of stack plumes before and after equilibrium with the atmosphere is attained.

(3) To develop techniques whereby an improved understanding of diffusion from large stack sources may be incorporated into the conventional models.

II. EXPECTED EFFECTS OF METEOROLOGICAL PARAMETERS ON THE SIZE AND SHAPE OF A RISING PLUME

A hot plume issuing from a smokestack is composed of turbulent gases possessing a mean vertical motion and buoyancy relative to the atmosphere. The turbulent nature of the flow induces immediate mixing with the environmental air. Further entrainment results from mechanical turbulence generated by the velocity shear between the plume and its surroundings. If there is a wind at the height of emission, the plume acquires horizontal momentum from the entrained air and rapidly bends over. In the bent-over stage, the efficiency of the mixing process is considerably enhanced[5], so that within a short distance, the stack gases have a horizontal component of velocity nearly equal to the wind speed. Photographic evidence, obtained in the wind tunnel studies of Halitsky, Randell, and Hackman[8], indicates that very near the stack exit, the plume's axis is inclined at an angle $\tan^{-1} u/w_o$ to the vertical. The plume continues to rise until its vertical momentum and density deficit are entirely dissipated. It can be easily demonstrated that for vertical velocities and temperatures typical of effluents from large modern power plants, the initial buoyancy is the major non-meteorological factor governing the extent of plume rise.

Priestley[9] argued that the rise, spread, and final diffusion of buoyant plumes ought realistically to be regarded in terms of three regimes, defined by changes in the relative importance of the various physical mechanisms involved. Initially, the entrainment process is governed by self-induced turbulence. Gradually, however, the impor-

tance of this mechanism diminishes, until at some point, atmospheric eddies begin to affect significantly the growth and rise of the plume. Normally this occurs before full rise is attained. When the buoyancy has completely decayed, the plume reaches equilibrium with its environment, and thereafter, the motions of the stack gases are completely indistinguishable from those of the atmosphere. The plume centerline is then determined by the mean wind, and any further widening or deepening of the plume must correspond exactly to turbulent fluctuations of the wind speed and direction. It is important to recognize that, in general, this will not be the case while the plume is rising.

In modelling the diffusion from a stationary, elevated source, it is standard practice to assume that all of the vertical and cross-wind spread of a plume may be explained in terms of the action of turbulent eddies upon an effluent which is initially in equilibrium with the atmosphere. This assumption is normally incorporated in the models by postulated a virtual point source at some estimated height directly above the true source. Thus, plume rise and diffusion are treated as separate phenomena. Such a procedure is unrealistic in that it disregards fundamental differences between the physical processes which govern a plume's growth before and after it attains equilibrium with the atmosphere. In so doing, it must also neglect the ways in which various meteorological conditions influence the development of a rising plume.

A principal concern of this study will be the entrainment during plume rise, and the sensitivity of this process to variations in local atmospheric conditions. Obviously, 'entrainment' is a suitable descrip-

tion for the turbulent diffusion which occurs subsequent to plume rise; but for clarity, the term will be used in this paper exclusively with reference to the growth of a rising plume. The term 'plume size' as employed throughout the following discussion, will denote some measure of the cross-sectional area of a plume in a plane normal to its mean horizontal travel. 'Plume shape' will refer to the relationship between the vertical and horizontal dimensions of such a cross section.

Observational data presented in later chapters suggests that even at short distances from the source, enormous differences in the size and shape of plumes can occur under different meteorological conditions. A major portion of this study is involved with determining relationships between appropriate measures of plume size and shape and specific meteorological parameters. The justification for this effort lies in the opportunity it may afford for determining the seriousness of discrepancies to be expected from diffusion schemes which employ the virtual point source approximation. Chapter V draws upon the results obtained in this analysis to propose a technique whereby the dependence of plume spread upon routinely available meteorological parameters may be incorporated within the diffusion models for large-source applications.

If it is agreed that entrainment in a rising plume may be legitimately studied in terms of size and shape characteristics, then the first requirement of the analysis is a rational selection of meteorological parameters in terms of which observed plume characteristics ought best to be explained. The variables chosen for this investigation are wind speed, directional wind shear, and the vertical profile of potential temperature. The following paragraphs discuss the physical

reasoning involved in selecting these parameters.

A. Wind speed

(1) The strength of the mean wind in the atmospheric layer occupied by the plume obviously plays a critical role in diluting the original vertical momentum of the stack gases. Each parcel of entrained air imparts its momentum to the plume; so that under conditions of strong winds, the mean motion of the plume must rapidly incline toward the horizontal. This means that the buoyancy of the hot effluent is effectively stretched downwind, and its density deficit is diminished at a lower height than would be the case with calm conditions. Briggs[5], in summarizing the results of numerous investigations, concludes that the relationship between plume rise and wind speed which best fits available data is

$$\Delta h \propto \bar{U}^{-1}$$

where Δh = plume rise above stack top,

$\bar{U}$ = mean wind speed at stack top.

(2) Superficially, it might be suggested that the rapid mixing of plume properties with those of the environment which occurs with high winds ought to result in a large cross section at some short downwind distance. In fact, the reverse is true. Stated simplistically, relatively few parcels of rapidly moving ambient air are required to effect the transport of plume material over a given distance. Thus, large plumes are to be expected with low wind speeds.

(3) The role of wind speed as an influence upon the vertical dimension of a plume cross section is rather complicated. High wind

speeds are characteristic of neutral and unstable conditions which favor vertical development. But, as noted above, strong winds inhibit the vertical motion of the plume as a whole, by diluting its buoyancy at low levels. In view of these counteracting processes, there is no reason to expect plume depth (and thus the shape, as defined above), to bear a strong correlation with wind speed.

B. Directional Wind Shear

A second meteorological parameter, which primarily affects cross-wind plume spread is the degree of directional shear of the wind in the layer of plume rise. Large vertical variations of wind direction act to laterally separate upper and lower sections of the plume, thereby increasing its overall width. It is anticipated, therefore, that the size of a plume cross section is positively related to the magnitude of the directional shear. Since directional shear bears no obvious relationship to plume depth, the expected correlation between this meteorological factor and plume shape (ratio of depth to width), is a negative one.

Care must be taken in efforts to parameterize directional shear. If it is defined as the vector difference between the winds at different levels, poor correlation with plume size may be expected, since such a definition incorporates a measure of the magnitude of the velocity in the layer. As discussed earlier, high values of directional shear should produce an effect on plume width opposite to that resulting from high wind speed. Consequently, in this paper directional shear is defined simply as the maximum angle through which the wind turns in the layer between stack top and plume centerline. This variable (or

the standard deviation of its range over some suitable time period), is the three-dimensional analogue to the σ_θ which often appears in the diffusion literature.

C. Vertical Potential Temperature Gradient

The vertical profile of potential temperature must exert the dominant influence upon the vertical spread of an entraining plume, since it is this profile which defines the static stability of the air which mixes with the plume gases. The entrainment process in stable air is characterized by the rapid decay of the plume's buoyancy; air entrained at low levels is carried aloft by the vertical momentum to regions of potentially warmer ambient air. In a neutral layer, the buoyancy of an individual element of plume gas remains constant, if the motion is considered adiabatic. Thus less rise is expected in a stable atmosphere.

In view of the damping influence of stability on plume rise, flat cross sections are anticipated with stable conditions. There is no apparent reason, however, to expect that the cross-sectional area of a plume will be correlated with stability.

III. MEASUREMENT DATA AND DATA REDUCTION

A. The LAPPES Data

The observational data which provide the basis for this investigation are the results of measurements performed in connection with the Large Power Plant Effluent Study (LAPPES), conducted by the U. S. Public Health Service during the period 1967-70. The sites chosen for the LAPPES project were the large coal-burning generating stations newly erected in the Chestnut Ridge area of western Pennsylvania. Extensive documentation of plumes from the 244-meter stacks at the Keystone and Homer City stations and the 305-meter stacks at the Conemaugh Station was coordinated with a comprehensive meteorological measurements program. Several features of the resulting data set render it particularly suitable for a study of the relationships between plume characteristics and atmospheric conditions: (1) Detailed information regarding plume cross-sectional sizes and shapes was obtained simultaneously with meteorological data defining the vertical structure of the atmospheric layer in which each plume was embedded. (2) The considerable extent of the volume of data collected enhances the credibility of any statistical properties which may emerge from its analysis. (3) The measurements were made in a predominantly rural area with fairly regular topography. This means that problems of background levels and terrain influences will be of minimal concern. (4) The primary emphasis of the LAPPES program was placed on observation of plume behavior in the morning hours prior to, and during the breakup of the stable ground layer. It is this period which is generally associated with maximum ground level concentrations, and is therefore of major concern in diffusion modelling.

The LAPPES data were tabulated in digitized form and are presented in three volumes[10]. Figure 1 provides an example of the data tabulations for October 24, 1968. The following section briefly describes the measurement techniques which were employed in the collection of the data. For specific instrumentation and procedural details the reader is referred to the LAPPES volumes.

(1) Plume Cross-Section Measurements

Horizontal traverses of the power plant plumes were made by instrumented helicopter at arc distances of 4.0, 10.0, and 16.0 km downwind from the stacks (1967 Keystone plumes were measured at 4.8, 10.0, and 16.0 km). Sulfur dioxide concentrations were continuously monitored during each pass through the plume, and usually, traverses were made at a sufficient number of elevations to define fairly precisely the top and bottom of the cross section. In this way, the spatial distribution of SO_2 within each cross section was determined, as well as reasonable estimates of the vertical and cross-wind dimensions. Tabulations of the measurements are presented in convenient form with instantaneous SO_2 readings at six-second intervals along each traverse, and coordinates fixing each measurement point with respect to the stack, as well as the height of each traverse.

(2) Meteorological Measurements

Pilot balloon measurements of winds aloft were conducted at the applicable power station whenever the cross-section measurements were in progress. Normally, the releases were made at half-hour intervals during each experiment. Wind speeds and directions at 50-meter height increments above the stack base were obtained from the original data by

Keystone #188 Arc 4.0 km
24 October 1968 Ref Pt 314°
0643-0704 EST SO_2 in pphm

Cum y (m)	Dir (°)	Traverse Height (m) 318	450	480	538	606	670	730	776	840	950	1010	1070	VIC
0	314.0					0								0
134	315.9	0	0			17		0		0				31
268	317.8	*6	*10			60		14		8				187
402	319.8	0	7	0		88		77		*60				419
536	321.7		2	12		*106		81		84			0	516
671	323.6		0	54	0	89		110		13		0	0	405
805	325.5			*120	2	102	0	*114	0	55	0	5	0	622
939	327.4			0	69	0	12	99	57	0	22	*33	0	463
1073	329.4				*180		31	17	22		46	0	0	516
1207	331.3				102		57	0	68		*58		0	496
1341	333.2				22		107		*69		18		0	358
1475	335.1				0		150		0		0		0	249
1609	337.1						*187							310
1743	339 0						115							191
1878	340 9						54							90
2012	342.8						10							17
2146	344.7						12							19
2280	346.7						0							0
CIC		20	70	665	1344	1654	2634	1836	773	789	516	136	0	
Peak		7	18	129	197	120	207	151	117	126	83	39	0	
Pass		4	5	3	2	1	6	7	8	9	10	11	12	

A. 4-Km Plume Cross Section

Keystone #2 24 October 1968

Time EST	Load (mw)	T (°C)	DT (°C)	Vel (mps)	SO_2 (g/s)	Cal/s x10⁶
0400	878	139	130	21.9	4133	31.4
0500	876	143	134	22.0	4108	32.2
0600	880	137	128	21.8	4133	30.9
0700	884	137	127	21.9	4158	30.9
0800	878	138	129	21.9	4133	31.2
0900	904	133	124	22.3	4259	30.7
1000	916	149	139	23.3	4309	34.8
1100	755	140	129	18.7	3553	26.8
1200	533	121	109	12.6	2495	15.9
1300						
1400						
1500						
1600						
1700						

B. Plant Operational Data

Ascn #K-1
24 Oct 68
0700 EST
Double

Z(m)	D(°)	S(mps)
Sfc		0.0
50	350.1	0.4
100	025.5	1.3
150	077.2	1.9
200	114.6	3.6
250	135.3	6.3
300	134.0	6.4
350	140.1	6.1
400	146.1	5.9
450	148.0	5.6
500	151.1	5.1
550	151.9	5.3
600	154.3	5.1
650	159.9	4.6
700	164.2	4.4
750	161.3	4.8
800	166.7	4.2
850	169.0	3.8
900	169.1	3.7
950	170.3	3.6
1000	171.6	3.2
1050	175.7	3.0
1100	185.6	2.6
1150	205.1	2.3
1200	216.2	2.4
1250	215.1	2.8

C. Pilot Balloon Ascent

Ascn #258
24 October 1968
0633 EST
Keystone

Z(m)	WB(°C)	T(°C)
Sfc	5.0	6.2
50	4.7	6.2
100	4.4	6.0
150	4.6	6.6
200	5.3	9.0
250	5.2	9.4
300	5.6	10.6
350	5.6	10.6
400	5.2	10.2
450	4.9	9.9
500	4.6	9.4
550	4.5	9.1
600	4.1	8.6
650	3.9	8.2
700	3.6	7.8
750	3.2	7.4
800	2.8	6.8
850	2.7	6.5
900	2.3	6.0
950	2.0	5.6
1000	1.8	5.2
1040	1.6	5.0

D. Helicopter Temperature and Wet Bulb Temperature Profile Measurements

Figure 1 Examples of Lappes Data Tabulations for Experiment at Keystone Station, October 24, 1968

interpolating between the 30-second readings.

On-site vertical profiles of wet-bulb and dry-bulb temperature were also measured at times corresponding to the plume SO_2 measurements. The soundings were made with helicopter-mounted sensors, and extended through the layer of plume rise. On most occasions, at least one such ascent was conducted within 30 minutes prior to or after a series of plume traverses. Wet-bulb and dry-bulb temperatures are tabulated at 50-meter intervals, usually commencing with surface values. Additional values were included, corresponding to significant levels such as the top or bottom of an inversion.

(3) Power Plant Operational Data

Hourly average values of important plant operational characteristics were computed and tabulated for the periods corresponding to measurements programs at a given site. Included are stack gas exit velocity and temperatures, SO_2 mass emission rate, and the heat flux at stack top. The significance of these data for the present study is solely as inputs to various plume rise formulae, and for mass balance calculations, as will be discussed below.

B. Selection of Cases for Analysis

This investigation is primarily concerned with the early stages of plume development. Therefore, only those cross sections measured at 4.0 or 4.8 km from the source are presently considered. Also, for simplicity, cases corresponding to the simultaneous operation of more than one stack unit at a power plant are disregarded. These comprise only a small number of measurements, and neither their inclusion with the cases corresponding to single stack operation, nor their examin-

ation separately is considered appropriate for present purposes.

If the LAPPES plume measurements are to be used to study plume sizes and shapes characteristic of various atmospheric conditions, it is essential to devise a technique by which the validity of the individual cross-section measurements may be assessed. It is to be expected that under some circumstances, such as suddenly shifting winds, the helicopter monitor may have failed to locate accurately the entire plume. Occasional equipment malfunctions and simple human judgement errors must also be considered as possible sources of inaccuracy. Since the reliability of these measurements is crucial to the success of this study, it is necessary to adopt some procedure for identifying unreliable data to avoid erroneous conclusions from the analysis.

The method employed to accomplish this objective is a simple mass balance calculation, comparing the flux of SO_2 through the area of the plume traversed with the known emission rate at the source. A numerical integration of the instantaneous concentrations along each horizontal pass through the plume was first performed. The cross-wind integrated concentrations at each traverse elevation were subsequently integrated over the measured vertical extent of the plume, and the resulting areal integrations then multiplied by the wind speed at the height of the observed plume centerline. This height was determined by the horizontal traverse corresponding to the highest crosswind-integrated concentration, and the wind speed at this level was obtained by interpolation from the appropriate pilot balloon ascent.

The ratio of the mass flux so computed, to the plant emission rate was calculated for each of the 119 cross-sections at 4.0 and 4.8 km.

This number of cases was slightly reduced by omitting those plume measurements for which concurrent wind and temperature profiles were missing. The values of the mass balance ratios vary from less than 0.1 to more than 0.9. Cases corresponding to very low ratios probably reflect difficulties in locating the plume. As such, these measurements may not be considered reliable ones on which to base conclusions relating meteorological factors to plume size and shape characteristics. It was tentatively decided to retain for study all cases corresponding to a mass balance of at least 0.5. None of the relatively few 4-km cross sections measured at the Conemaugh Station met all the above criteria. The delimiting value of 0.5, although somewhat arbitrary, was chosen in view of recent European studies of the atmospheric oxidation of sulfur dioxide to $SO_4^=$. Weber[11] found that a half-life of 30 minutes may be realistic for SO_2 stack emissions. This corresponds roughly to the travel time over 4 km with speeds of about 2 m/sec, the lowest values encountered during the LAPPES experiments. Appendix I includes an investigation of possible manifestations of this chemical decay in the LAPPES plume data. The variations of the mass balance ratio with wind speed and relative humidity are discussed in this context.

As a further precaution, the remaining data set was divided into two nearly-equal groups of cross-section measurements. Those corresponding to a ratio of 0.7 or higher (ratio of integrated plume SO_2 content to stack emission), were designated Class A plumes. The others, with ratios in the range between 0.5 and 0.7 were termed Class B plumes. Statistical correlations between plume dimensional characteristics and specific meteorological parameters were initially evaluated separately

for each class in order to determine whether significant differences occurred. In addition, such correlations were also determined separately for the Keystone and Homer City plumes, so that local effects, such as terrain features, would not influence the results. As discussed in the next chapter, nearly identical statistical properties were found for Class A and B plumes. Similarly, no important differences were revealed in the results obtained at the individual power plant sites. Thus, for purposes of further analysis, these classifications were disregarded. As a result, a data set of 58 equally-weighted cross sections was retained.

IV. ANALYSIS OF PLUME CROSS SECTIONS AT 4 AND 4.8 KM

A. Measures of Plume Size and Shape

In order to facilitate comparisons with results obtained elsewhere, the dimensions of a plume cross section will be expressed in terms of σ_y and σ_z, respectively, the standard deviations of the horizontal and vertical concentration distributions (assumed Gaussian). The determination of the plume edge is somewhat arbitrary, since it depends entirely upon the sensitivity of the device used to measure SO_2 concentration. For this reason, it is often convenient to define the edge as the locus of points at which the measured SO_2 concentration is just 1/10th of the central (maximum) value. It is a property of the normal distribution that the 1/10th value is found at a distance of 2.15 standard deviations from the point corresponding to the maximum. Thus, the total width of a plume is approximated by $4.30\sigma_y$, and the depth by $4.30\sigma_z$.

A brief inspection of the LAPPES 4-km plume cross sections indicates that in every case, the width is substantially larger than the vertical extent. This is a reflection of the limitations imposed by the surface boundary upon the development of vertical eddies, augmented by the fact that stable conditions prevailed during most of the measurement experiments. The cross sections are thus elliptical in shape, and their areas may be approximated by $\pi(2.15)^2\sigma_y\sigma_z = 14.52\sigma_y\sigma_z$. The product $\sigma_y\sigma_z$ is thus a valid indicator of plume size. Similarly, the ratio of the axes of the idealized ellipse, σ_z/σ_y, provides a convenient parameterization of plume shape.

B. Plume Characteristics at 4 km and 4.8 km

The LAPPES 4-km and 4.8-km cross-section tabulations provide instantaneous SO_2 concentrations along each traverse at six-second intervals. This corresponds to measurements every 134 m with a helicopter speed of 50 mph, or 107 m with a speed of 40 mph. Cross-wind integrations at each height traversed and vertical integrations at each lateral distance from the plume axis are also provided (see Figure 1). The upper and lower elevations corresponding to 10% maximum values were determined by interpolation between the cross-wind integrations. By a similar process of interpolation between the vertical integrations, the lateral distances from the axis to 10% maximum readings were obtained. These distances are $2.15\sigma_y$ and $2.15\sigma_z$ as explained above. Thus, the values of σ_y and σ_z as well as the size and shape parameters $\sigma_y\sigma_z$ and σ_z/σ_y were computed and recorded for all Class A and B plumes.

Virtually all commonly-employed point-source diffusion models incorporate the assumption of a Gaussian distribution of effluent concentrations within a plume cross section. It is not the purpose of this study to prove or disprove the validity of this approximation. It is, however, important to determine whether the use of the shape parameter σ_z/σ_y introduces significant distortions as a representation of actual plume shape. The LAPPES data allow a fairly precise definition of the actual horizontal and vertical extents of each plume. Interpolation of the cross-wind and vertically integrated concentrations can be used to locate the probable points of zero concentration based on the gradients near the edge of the measured cross sections. Thus, values of the total plume width W and depth D are easily obtained. Figure 2 is a plot of

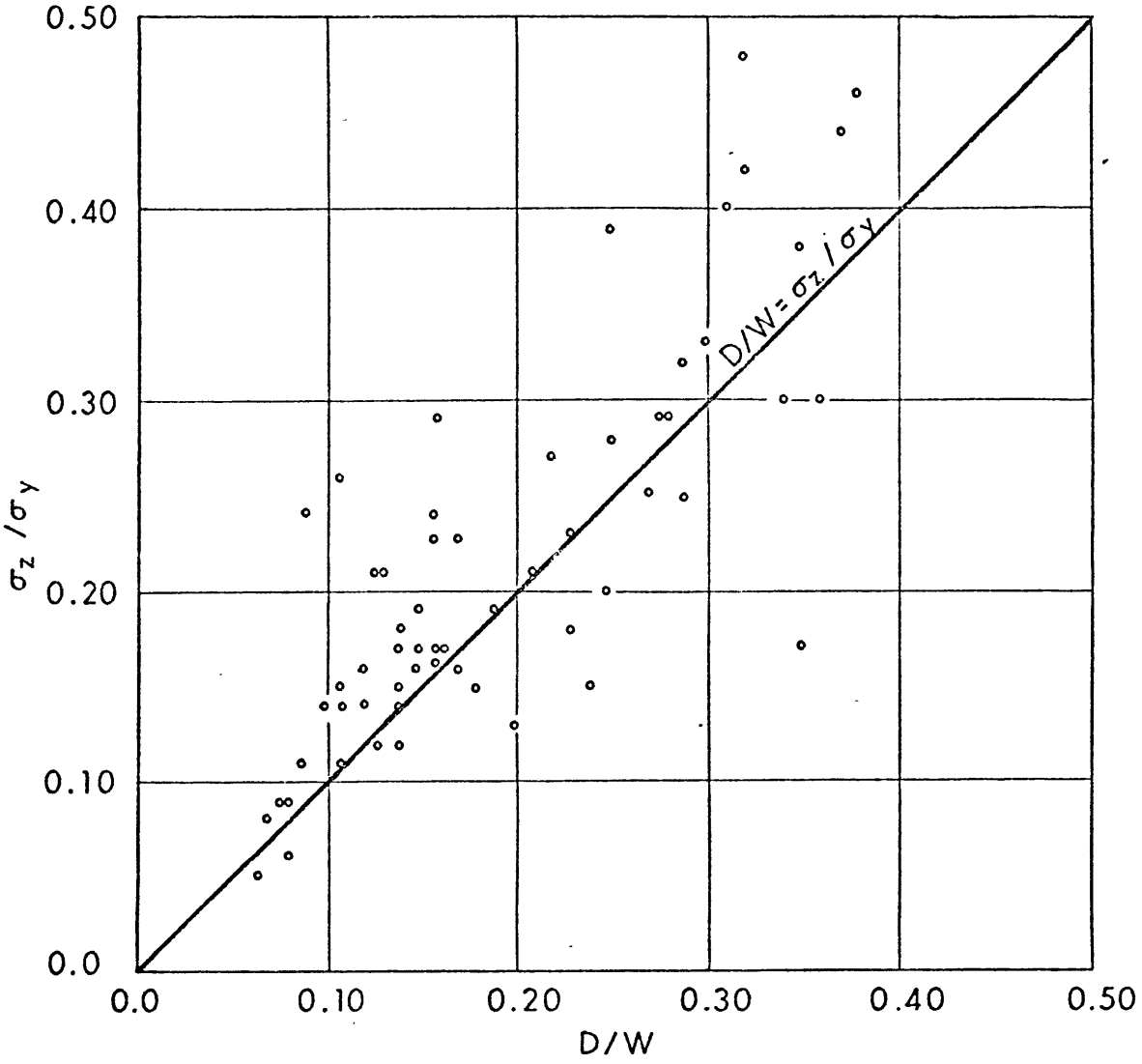

Figure 2 Comparison of Actual Ratio of Plume Depth, D to Plume Width, W with Gaussian Parameter σ_z/σ_y

the values of D/W vs. the shape parameter σ_z/σ_y. Excellent agreement is seen, assuring the validity of the parameterization for plume shape adopted in this investigation.

Meteorological data corresponding to each cross section were obtained from the most nearly concurrent pilot-balloon ascent and helicopter temperature sounding. In cases where two balloon releases were made at the approximate time of a plume measurement experiment, the wind speeds and directions at any height were taken as the average values obtained during the two ascents. A similar technique of averaging two temperature profiles was employed where appropriate.

Tables 1 and 2 display the dimensional characteristics of Class A and B plumes with the corresponding values of the three meteorological parameters discussed in Chapter II. In the tables $\bar{U}$ is the mean wind speed in the column between 250 m above stack base (stack tops are at 244 meters), and the apparent plume centerline. 'A' represents the directional shear, i.e. the maximum angle, expressed in radians, through which the wind turns in this layer. The stability parameter, $\partial\theta/\partial z$ is the average gradient of potential temperature in the same layer. Near the surface, $\frac{\partial\theta}{\partial z} \approx \frac{\partial T}{\partial z} + \Gamma$, where Γ is the dry adiabatic lapse rate. Thus, the values of $\partial\theta/\partial z$, expressed in $^{\circ}C/100\,m$, are simply the values of $\partial T/\partial z + 1$.

It is obvious from inspection of Tables 1 and 2 that the cross-wind and vertical plume dimensions at a given downwind distance depend in a complicated way upon the values of wind speed, directional shear, and stability. While the actual diffusion process is governed by simultaneous non-linear interactions between plume gases and their atmos-

Table 1

Size and Shape Parameters of Plume Cross Sections at 4.0 and 4.8 km Downwind with Corresponding Meteorological Data

Class A Plumes*

Case No.	Plant	Downwind Distance (km)	Date	EST	σ_y (meters)	σ_z (meters)	$\sigma_y\sigma_z$ ($m^2 \times 10^3$)	σ_z/σ_y	A (radians)	$\bar{U}$ (m/sec)	$\partial\theta/\partial z$ (°C/100m)
1	Keystone	4.8	10/21/67	0715-0727	291	80	23.216	.27	0.23	13.15	+0.5
2			10/24	0711-0728	380	62	23.506	.16	1.06	7.13	+1.7
3			10/27	0711-0728	143	33	4.649	.23	0.33	8.70	+1.3
4			10/31	0702-0714	320	35	11.117	.11	0.56	6.10	+2.7
5		4.0	3/18/68	0931-0947	413	96	39.648	.23	0.59	9.15	+0.68
6			3/20	0702-0713	200	59	11.822	.30	0.31	9.50	+0.10
7			4/01	0658-0717	361	106	38.410	.29	0.17	19.00	+0.15
8			5/06	0600-0617	586	64	37.738	.11	0.38	6.95	+0.85
9			5/07	0553-0607	160	76	12.240	.48	0.08	7.50	+1.60
10			5/08	0600-0611	293	51	14.900	.17	0.25	10.25	+0.90
11			5/09	0822-0838	348	85	29.676	.25	0.07	12.35	+0.60
12			5/27	0615-0640	234	106	24.916	.46	0.33	12.7	+0.20
13			7/04	0642-0659	558	65	173.075	.12	0.41	4.25	+0.72
14			7/21	0555-0631	1482	81	119.613	.05	1.50	2.65	+0.73
15			10/24	0643-0704	411	122	50.384	.30	0.43	5.45	+0.70
16			4/09/69	0653-0706	271	41	11.065	.15	0.42	10.05	+0.75
17			4/10	0708-0728	292	89	26.126	.30	0.11	12.65	+0.24
18			4/14	0656-0719	653	57	37.385	.09	0.88	4.15	+1.80
19			4/14	1048-1118	625	84	52.775	.13	0.86	2.85	+0.22
20			4/15	0655-0712	293	44	12.935	.15	0.48	6.90	+0.48
21			4/17	0657-0724	419	102	42.905	.24	0.13	7.90	+1.35
22			10/10	0650-0702	443	55	24.188	.12	0.40	8.95	+1.50
23			10/29	0732-0742	435	26	11.340	.06	0.06	8.45	+1.10
24			10/30	0727-0748	423	58	24.686	.14	0.60	6.20	+1.52
25	Homer City	4.0	10/15/69	0751-0817	646	56	37.296	.09	0.52	3.40	+0.72
26			10/18	0710-0725	267	65	17.355	.24	0.43	12.15	+1.40
27			10/21	0657-0714	315	100	31.480	.32	0.19	12.30	+0.28
28			10/24	0700-0724	443	71	31.710	.16	0.57	5.05	+0.44
29			4/21/70	0703-0720	292	55	16.148	.19	0.09	16.75	+0.10
30			5/12	0649-0704	328	57	18.609	.17	0.15	7.2	+0.60
31			5/15	0810-0837	563	105	59.080	.19	0.47	9.7	+1.13
32			11/09	0704-0729	219	85	18.544	.39	0.01	10.5	+0.60

*Class A plumes defined by $R \geq 0.70$.

R = ratio of cross-section integrated SO_2 mass flux to plant SO_2 emission rate.

σ_y = standard deviation of crosswind SO_2 distribution.

σ_z = standard deviation of vertical SO_2 distribution.

$\sigma_y\sigma_z$ = size parameter.

σ_z/σ_y = shape parameter.

A = directional shear = maximum angle through which wind turns in the layer between stack top and cross-section centerline.

$\bar{U}$ = mean wind speed in the layer between stack top and cross-section centerline.

$\frac{\partial\theta}{\partial z}$ = mean vertical potential temperature gradient.

Table 2

Size and Shape Parameters of Plume Cross Sections at 4.0 and 4.8 km Downwind with Corresponding Meteorological Data

Class B Plumes*

Case No.	Plant	Downwind Distance (km)	Date	EST	σ_y (meters)	σ_z (meters)	$\sigma_y\sigma_z$ ($m^2 \times 10^3$)	σ_z/σ_y	A (radians)	$\bar{U}$ (m/sec)	$\partial\theta/\partial z$ (°C/100m)
33	Keystone	4.8	10/23/67	0713-0731	599	46	27.295	0.08	0.98	6.35	+1.65
34			10/26	0715-0736	199	83	16.508	0.42	0.17	10.10	+0.17
35			10/28	0710-0722	252	73	18.381	0.29	0.16	6.70	+0.47
36			10/29	0704-0719	306	64	19.655	0.21	0.97	4.05	+0.50
37		4.0	3/15/68	1007-1033	334	127	42.310	0.38	0.10	11.70	+0.30
38			5/05	0834-0905	617	142	87.756	0.23	0.48	7.05	+0.31
39			5/09	0553-0604	246	63	15.521	0.26	0.32	12.55	+1.15
40			5/10	0641-0657	184	81	14.886	0.44	0.12	5.25	+0.72
41			5/11	0605-0621	295	86	25.283	0.29	0.21	5.05	+1.00
42			5/26	0545-0605	361	59	21.359	0.16	0.87	6.85	+1.90
43			10/20	0634-0645	149	21	3.167	0.14	0.31	7.80	+1.30
44			10/22	0643-0655	370	78	28.823	0.21	0.61	6.10	+1.80
45			10/26	0656-0713	226	74	16.650	0.33	0.30	11.35	+0.50
46			10/30	0735-0750	281	48	13.343	0.17	0.19	7.85	+0.68
47			10/31	0841-0916	733	118	86.567	0.17	0.91	2.65	+0.52
48			4/11/69	0708-0744	422	169	71.615	0.40	0.38	4.05	+0.09
49			4/28	0644-0653	224	40	8.892	0.18	0.07	13.65	+0.60
50			10/09	0652-0709	519	73	37.702	0.14	0.52	6.55	+0.72
51			10/31	0723-0735	262	41	10.838	0.16	0.52	8.30	+1.67
52			11/01	0801-0816	369	64	23.450	0.17	0.09	11.70	+0.30
53	Homer City	4.0	10/11/69	0648-0703	345	49	16.767	0.14	0.41	7.95	+1.30
54			10/13	0648-0706	331	71	23.501	0.21	0.14	9.00	+0.95
55			10/17	1017-1030	343	50	17.150	0.15	0.09	13.90	+0.20
56			10/20	0644-0700	298	61	18.267	0.20	0.09	14.15	+0.70
57			11/06	0732-0758	420	116	48.720	0.28	0.19	11.20	-0.13
58			5/11/70	0839-0858	437	67	29.323	0.15	0.56	5.15	+0.52

* Class B Plumes defined by $0.50 \leq R < 0.70$

R = ratio of cross-section integrated SO_2 mass flux to plant SO_2 emission rate.

σ_y = standard deviation of crosswind SO_2 distribution.

σ_z = standard deviation of vertical SO_2 distribution.

$\sigma_y\sigma_z$ = size parameter.

σ_z/σ_y = shape parameter.

A = directional shear = maximum angle through which wind turns in the layer between stack top and cross-section centerline.

$\bar{U}$ = mean wind speed in the layer between stack top and cross-section centerline.

$\frac{\partial\theta}{\partial z}$ = mean vertical potential temperature gradient.

pheric environment, it is reasonable to assume that a linear regression analysis relating specific size or shape parameters to individual meteorological variables may provide useful indications of the relative importance of, for example, the effect of wind speed on plume width, etc. A series of such regression analyses was performed and the associated correlation coefficients are tabulated in Table 3. Correlation coefficients were evaluated separately for Keystone Class A and B cross sections at 4.0 km. Only eight cross-section measurements at 4.8 km were available. It was not considered appropriate to examine separately the statistical properties of so small a data set, nor to include it with measurements obtained at a shorter downwind distance. Comparisons of the Class A and B correlations indicate that essentially the same dependence of size-shape parameters on meteorological factors obtain for both sets of measurements; i.e. Class A and B plume measurements are equally valid for the purposes of this investigation. Correlation coefficients for the combined classes were thus computed and in subsequent discussions the A-B classification is entirely disregarded. In addition, coefficients for all combined Class A and B Homer City plume measurements were computed and are also presented in Table 3. No significant differences in the statistics obtained at the two sites are apparent.

Table 3 indicates a persistent negative correlation between plume depth and atmospheric stability. This result was anticipated and conforms to the accepted practice of assigning a small deepening rate under stable conditions (e.g. Turner's E and F curves for σ_z).

The table also indicates a quite definite negative relationship

Table 3

Keystone and Homer City 4-km Cross-Sections:
Linear Correlation Coefficients between Plume Size-Shape Characteristics and Specific Meteorological Variables

X	Y	CORRELATION COEFFICIENTS			
		Keystone Class A*	Keystone Class B*	Keystone Class A & B Combined	Komer City Class A & B Combined
Number of Cases →		20	16	36	14
$\bar{U}$	σ_y	-0.57	-0.49	-0.51	-0.63
$\partial\theta/\partial z$	σ_y	0.005	-0.24	-0.05	-0.03
A	σ_y	0.74	0.63	0.68	0.68
$\bar{U}$	σ_z	0.34	-0.38	-0.03	0.40
$\partial\theta/\partial z$	σ_z	-0.56	-0.51	-0.54	-0.41
A	σ_z	-0.36	0.01	-0.08	-0.25
$\bar{U}$	$\sigma_y\sigma_z$	-0.46	-0.50	-0.47	-0.15
$\partial\theta/\partial z$	$\sigma_y\sigma_z$	-0.20	-0.49	-0.34	-0.21
A	$\sigma_y\sigma_z$	0.50	0.41	0.42	0.34
$\bar{U}$	σ_z/σ_y	0.55	0.04	0.36	0.65
$\partial\theta/\partial z$	σ_z/σ_y	-0.23	-0.38	-0.29	-0.23
A	σ_z/σ_y	-0.55	-0.61	-0.57	-0.70

*Class A and B plumes as defined in Tables 1 and 2.

X = meteorological variable.
Y = plume size or shape characteristic.
All variables as defined in Tables 1 and 2.

between plume width and wind speed. This is an important result. In modelling the diffusion from stack sources it is common practice to assume an inverse proportionality between $\bar{U}$ and effluent concentration at any downwind point. The justification offered in support of this assumption is that high wind speeds tend to increase the separation between successively emitted portions of plume material along the mean wind direction. With low wind speeds, this separation is smaller, leading to the conclusion that downwind concentrations should be largest for this case. Such an argument is strictly valid only in a uniform flow field. Common experience has shown that persistent wind directions normally occur with strong winds under the influence of well-defined synoptic-scale systems (e.g. deep cyclones). Variability in the direction of the wind is associated with low wind speed, generally in the absence of such synoptic systems. What Table 3 dramatically demonstrates is that very low wind speeds, and hence, variability in the wind direction, produce large, diffuse plumes at a given downwind distance. High wind speeds result in narrow, concentrated cross sections.

The high positive correlation between directional shear and plume width is entirely consistent with this argument. A wide angular turn of the wind in the layer of plume rise laterally separates portions of the plume at different heights. As will be demonstrated presently, this effect is greatest when wind speeds are low. There are two reasons for this. First, low winds characteristically exhibit directional variability in the vertical as well as at a particular level. Secondly, low speeds favor large plume rise; thus, under these conditions the plume passes through a deeper atmospheric layer with a consequent increase in the

directional shear.

To clarify further the combined effects of meteorological parameters upon plume dimentions, plots of those relationships corresponding to meaningful correlation coefficients are presented in Figures 3-5. Examination of these figures affirms the ambiguous nature of the relationships between plume dimensions and individual meterological variables, although in Figure 5, a near-linear variation of plume width with directional shear is exhibited. In view of the interrelationships between the variables, the plume data were sub-classified into groups corresponding to distinct ranges of wind speed and stability in Figures 3-5.

C. Comparisons of Observed Plume Dimensions with the Turner Diffusion Coefficients

It is desirable to express diffusion coefficients in terms of the smallest possible number of meteorological variables. For practical applications it is also important for these variables to be ones routinely available from synoptic observations. With the advantages of reducing the number of atmospheric parameters in mind, a series of correlation coefficients were computed for all combinations of the three meteorological parameters discussed previously (see Table 4). A large negative correlation is seen to exist between wind speed and directional shear. Thus, to a first approximation, knowledge of wind speed in the plume rise layer amounts to knowledge of the vertical variability of wind direction. This important fact permits the use of a classification scheme based upon wind speed and stability only.

It is of considerable interest to compare the values of σ_y and

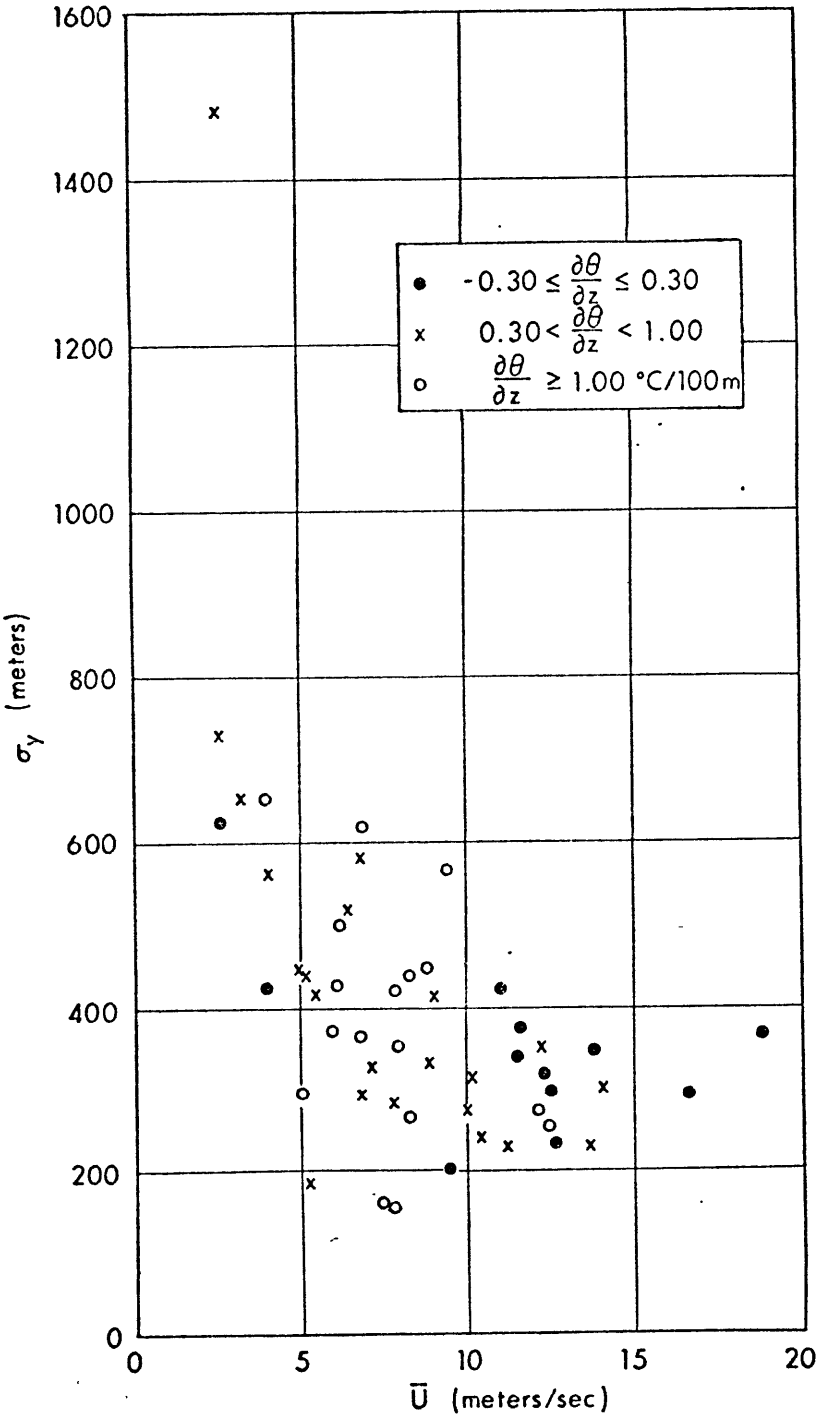

Figure 3 Class A and B Plumes: Keystone and Homer City 4-Km Cross Sections. Variation of Plume Width Parameter, σ_y with Mean Wind Speed, U

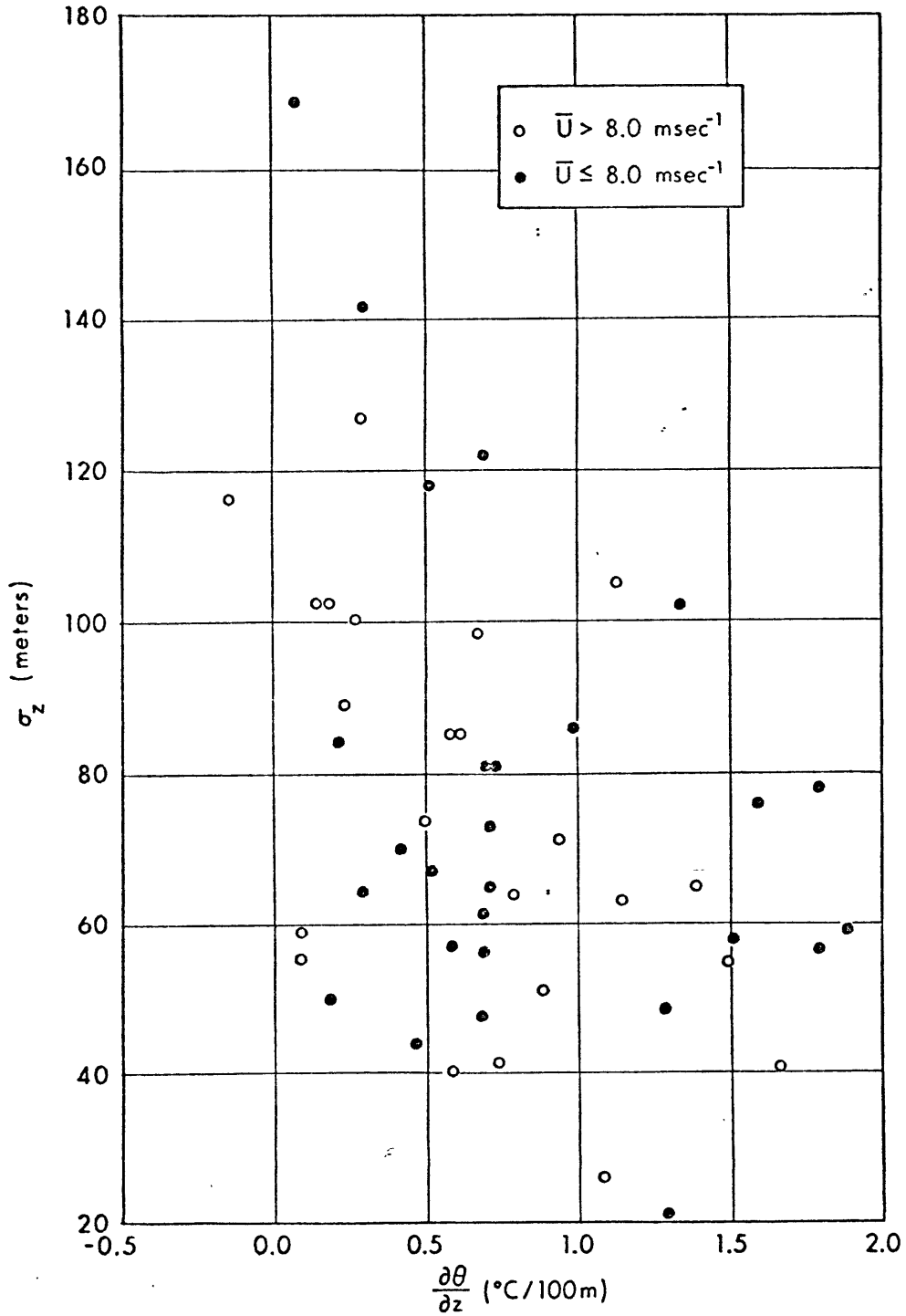

Figure 4 Class A and B Plumes: Keystone and Homer City 4-Km Cross Sections. Variation of Plume Depth Parameter σ_z with Stability Parameter $\partial\theta/\partial z$

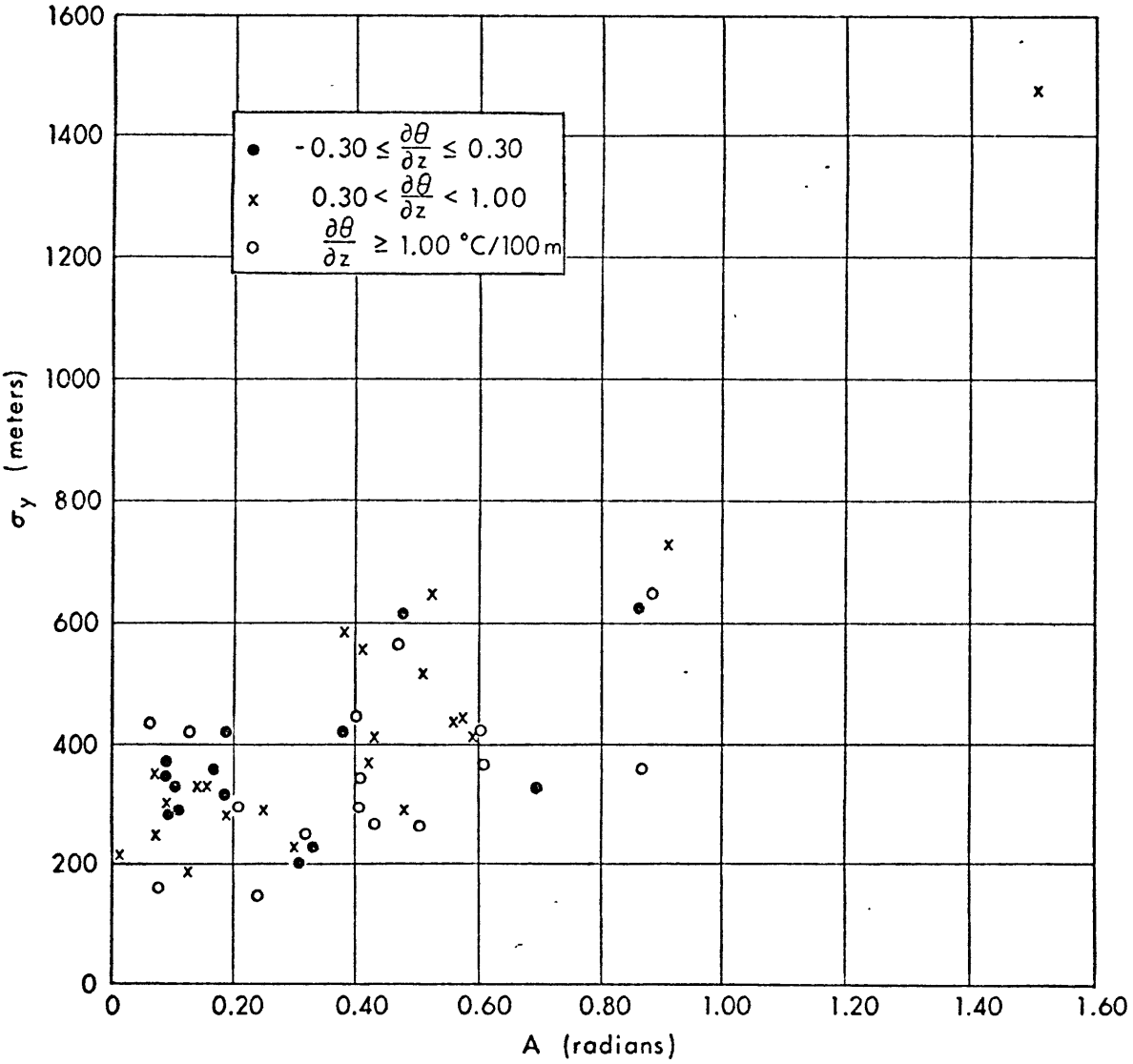

Figure 5 Class A and B Plumes: Keystone and Homer City 4-Km Cross Sections. Variation of Plume Width Parameter, σ_y with Wind Directional Shear Parameter, A

Table 4

Keystone and Homer City Sites:
Linear Correlations Between Specific Meteorological Parameters during 4-km Plume Cross-Sectional Measurements

		CORRELATION COEFFICIENTS			
X	Y	Keystone Class A	Keystone Class B	Keystone Class A & B Combined	Homer City Class A & B Combined
Number of Cases		20	16	36	14
$\overline{U}$	$\partial\theta/\partial z$	- 0.42	-0.09	-0.28	0.07
$\overline{U}$	A	- 0.65	-0.52	-0.60	-0.66
A	$\partial\theta/\partial z$	0.12	0.47	0.27	0.22

X, Y = meteorological variables.

$\overline{U}$ = mean wind speed in plume rise layer.

$\frac{\partial\theta}{\partial z}$ = mean vertical potential temperature gradient in plume rise layer.

A = directional shear in plume rise layer.

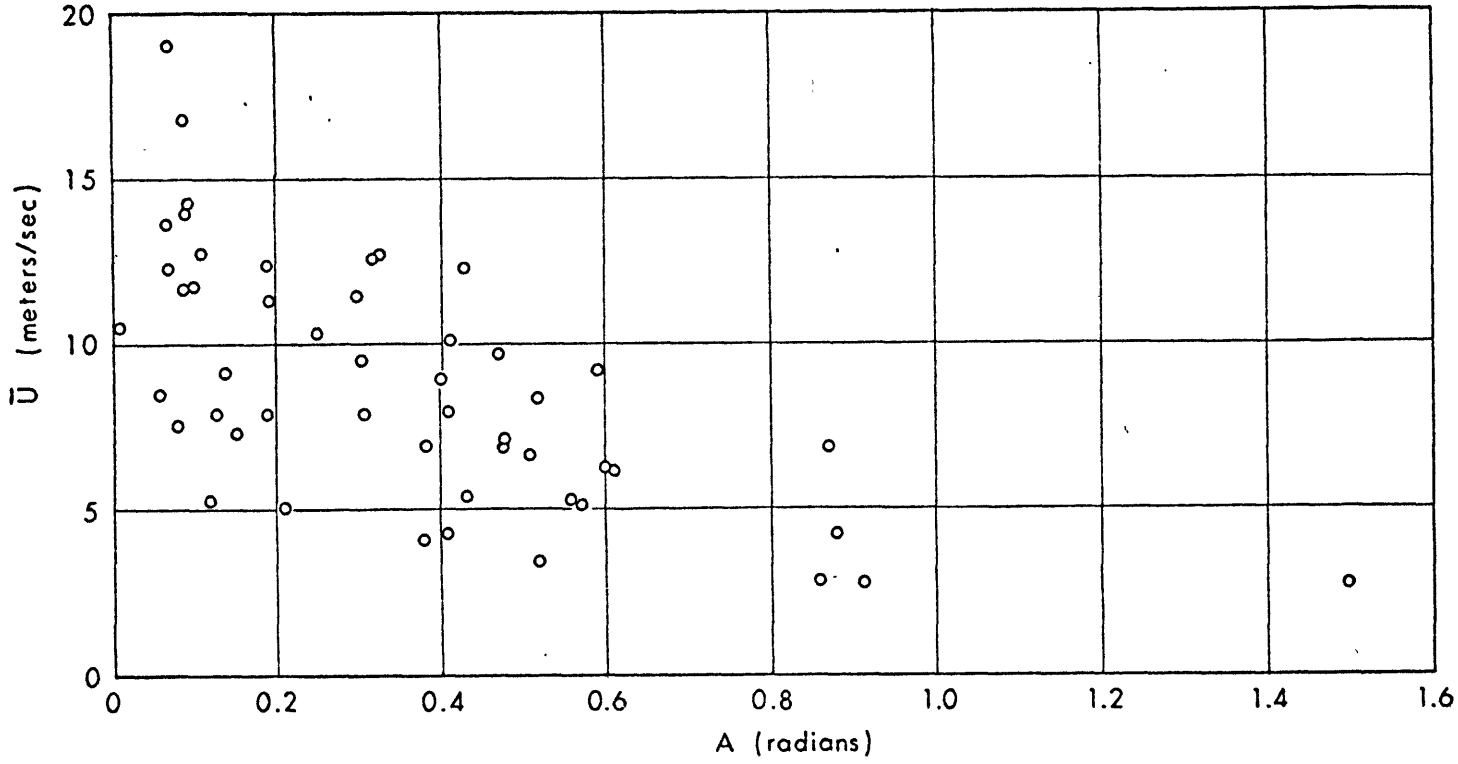

Figure 6 Wind Measurements at Keystone and Homer City Plants.
Mean Wind Speed, U vs. Directional Shear, A

σ_z from the 4-km cross-section measurements with those to be expected at this distance from the Turner dispersion model[4]. For this purpose it is convenient to group the data into classes corresponding to similar atmospheric conditions. Three ranges of stability were chosen to represent near-neutral, moderately stable, and very stable conditions. The average value of $\bar{U}$ for the cases included in Tables 1 and 2 is about 8 m/sec. Each stability was therefore divided according to whether the wind speed was greater or less than this mean value. Average values of σ_y, σ_z, and σ_z/σ_y were calculated for each of the six meteorological categories. The results are presented in Table 5. Included below are Turner's 4-km values of σ_y and σ_z corresponding to the four most stable categories, ranging from slightly unstable to very stable.

It is difficult to compare stability classifications defined, as has been done here, by a knowledge of the actual vertical temperature profile, with those defined by Turner in terms of solar insolation and wind speed near the ground. However, it is certain that the true static stability of the atmosphere ranged from neutral to very stable during the LAPPES measurements. Inspection of Table 5 indicates that the use of Turner's model with stability categories D, E, or F would widely underestimate both the vertical and cross-wind extent of the LAPPES plumes in the great majority of cases.

Entrainment into the rising plume produces a greater plume depth and width than would be obtained by applying Turner's curves for a point source directly above the stack. If the virtual point source is to remain above the true source, then an accurate simulation of the entrainment with this model must assume a stability category more unstable

Table 5

Keystone and Homer City Plants:
Average Values of Plume Dimensional Characteristics at
4 km for Six Classifications by Wind Speed and Stability

		Stability (°C/100m)	Windspeed	$\overline{\sigma_y}$(m)	$\overline{\sigma_z}$(m)	$\overline{\sigma_z/\sigma_y}$
NEAR-NEUTRAL	1	$-0.3 < \frac{\partial\theta}{\partial z} < 0.3$	$\overline{U} \geq$ 8mps	308	85	0.28
	2	$-0.3 < \frac{\partial\theta}{\partial z} < 0.3$	$\overline{U} <$ 8mps	523	126	0.24
MODERATELY STABLE	3	$0.3 \leq \frac{\partial\theta}{\partial z} < 1.0$	$\overline{U} \geq$ 8mps	302	71	0.23
	4	$0.3 \leq \frac{\partial\theta}{\partial z} < 1.0$	$\overline{U} <$ 8mps	464	80	0.17
VERY STABLE	5	$\frac{\partial\theta}{\partial z} \geq 1.0$	$\overline{U} \geq$ 8mps	369	59	0.16
	6	$\frac{\partial\theta}{\partial z} \geq 1.0$	$\overline{U} <$ 8mps	348	67	0.19

Turner's Values for σ_y, σ_z, σ_z/σ_y at 4 km

Class C SLIGHTLY UNSTABLE	Class D NEUTRAL	Class E MODERATELY STABLE	Class F VERY STABLE
$\sigma_y \sim 370$ m	$\sigma_y \sim 246$ m	$\sigma_y \sim 183$ m	$\sigma_y \sim 122$ m
$\sigma_z \sim 218$ m	$\sigma_z \sim 77$ m	$\sigma_z \sim 50$ m	$\sigma_z \sim 31$ m
$\sigma_z/\sigma_y \sim 0.59$	$\sigma_z/\sigma_y \sim 0.31$	$\sigma_z/\sigma_y \sim 0.27$	$\sigma_z/\sigma_y \sim 0.25$

than that indicated by the vertical temperature structure. The discrepancies are greater for the values of σ_y than for σ_z. Also note that agreement is generally poorer with low wind speeds. Except for very stable atmospheres, a crude fit with observed σ_y's could be obtained with the model by assuming the next most unstable category when wind speeds are high. With light winds, however, a shift of at least two categories would be necessary. Under very stable conditions, observed values of σ_y appear to be insensitive to wind speed.

It is to be expected that the apparent underestimation of plume size by the Turner model should lead to substantial overpredictions of ground-level SO_2 concentrations for neutral and stable situations. Unfortunately, the data sample does not include the typical "B" stability condition of wind speeds $\leq$ 5 m/sec and an unstable lapse rate. This meteorological situation is ordinarily associated with the highest ground-level concentrations for an elevated source. It would be desirable to determine whether the usual application of the Turner model is also underestimating plume size (and thus, overestimating ground-level concentrations), in such situations.

D. Summary

It has been seen in this chapter that the strong negative correlation between directional shear and wind speed is of primary importance in determining the cross-sectional size of entraining plumes. Doubt has been cast upon the traditional assumption of inverse proportionality between wind speed and the downwind concentrations associated with buoyant effluent released from tall stacks. Especially when winds are light, models which assume diffusion from a point source directly

above the stack widely underestimate the rate of growth of stack plumes. In the next chapter, it will be shown that the introduction of a virtual point source upwind from the true source may be used to improve the predictive capabilities of conventional models for tall stack applications.

V. ANALYSIS OF PLUME RISE AND ENTRAINMENT WITH LAPPES DATA

A. Plume Rise

Briggs[5] utilized a form of the entrainment hypothesis proposed by Taylor[7] to solve a simplified set of differential equations representing mass continuity, conservation of buoyancy, and conservation of momentum, arriving at a workable model of plume rise. Briggs chose constants of integration to obtain good agreement with plume rise data from a large number of previous studies encompassing a wide range of stack heights and initial conditions. More will be said concerning the Taylor entrainment assumption in the next section of this chapter.

For the case of primary interest in the present context, i.e. a buoyant plume in a cross wind, the plume rise formula developed by Briggs is expressed by

$$\Delta h = 1.6F^{1/3}U^{-1}X^{2/3} \qquad (1)$$

where: F is the initial flux of the buoyant force divided by

$$\pi\rho \approx 3.7\times10^{-5}\ \frac{m^4 sec^{-3}}{cal/sec}\ Q_H,$$

U = mean wind speed,

X = downwind distance, and

Q_H = heat emission due to stack efflux.

This formula is recommended for use up to the downwind distance corresponding to full rise which is given approximately for neutral conditions[12] by

$$X_{max} = 119F^{2/5}\ , \qquad (2)$$

and for stable conditions by

$$X_{max} = 2.4Us^{-\frac{1}{2}} \tag{3}$$

where s is the stability parameter $\frac{g}{T}\frac{\partial\theta}{\partial z}$.

Thus, the height of final rise is given directly by eq. (1) for neutral stability, and for stable air by

$$\Delta h_{max} = 2.9\left(\frac{F}{Us}\right)^{1/3} \tag{4}$$

The LAPPES plume cross-section measurements at 4 km are well beyond the point of maximum rise. Thus, the height of the cross-section centerlines above stack top provide a good estimate of Δh_{max} for each case. In addition, the distance from the stack to the point of maximum rise, X_{max}, can be computed using the known values of stability, wind speed, and heat emission corresponding to each cross section.

Some uncertainty exists as to the most appropriate formula for computing plume rise in cases where the stability is stable but near neutral. Consequently, plume rise was initially calculated using both equations (1) and (4) for each case. The best fit with the LAPPES data was obtained with (4) when $\frac{\partial\theta}{\partial z} \geq 0.30\ \frac{^{\circ}C}{100m}$. Table 6 present comparisons of the calculated plume rise values with the observed 4-km and 4.8-km centerline heights above stack top. Although there are large errors in predicting plume rise for individual cases, on the average, the Briggs formulae give remarkably accurate results, considering the range of temperature gradient and mean wind speed over the 58 cases (see box at end of Table 6). Briggs recommends the use of eq. (4) for layers of 'uniform' stability; and referring back to the original data, it is found that such cases are indeed the ones for which the

Table 6

Calculated and Observed Plume Rise
4.8 and 4.0 km Cross Sections

Case No.	Plant	Downwind Distance (km)	Date	$\partial\theta/\partial z$ ($\frac{°C}{100m}$)	$\bar{U}$ (mps)	X_{max} (meters)	$2.9(\frac{F}{Us})^{\frac{1}{3}}$ stable (meters)	$1.6F^{\frac{1}{3}}\bar{U}^{-1}X^{\frac{2}{3}}$ neutral (meters)	observed plume rise (meters)	Ratio of observed to calculated plume rise neutral	stable
1	Keystone	4.8	10/21/67	+0.50	13.15	2386	175		234		1.34
2			10/24	+1.7	7.13	707	185		203		1.10
3			10/27	+1.3	8.70	978	164		176		1.07
4			10/31	+2.7	6.10	481	146		122		0.84
5		4.0	3/18/68	+0.68	9.15	1226	198		250		1.26
6			3/20	+0.10	9.50	1759		231	218	.94	
7			4/01	+0.15	19.00	1805		119	213	1.79	
8			5/06	+0.85	6.95	978	220		199		0.91
9			5/07	+1.60	7.50	757	175		111		0.63
10			5/08	+0.90	10.25	1397	197		120		0.61
11			5/09	+0.60	12.35	2070	199		139		0.70
12			5/27	+0.20	12.70	1894		195		.77	
13			7/04	+0.72	4.25	648	282		309		1.10
14			7/21	+0.73	2.65	406	244		441		1.81
15			10/24	+0.70	5.45	839	276		426		1.54
16			4/09/69	+0.75	10.05	1516	208		214		1.03
17			4/10	+0.24	12.65	1947		203	266	1.31	
18			4/14(1)	+1.80	4.15	401	226		134		0.59
19			4/14(2)	+0.22	2.85	2113		1017	646	0.64	
20			4/15	+0.48	6.90	2057	299		271		0.91
21			4/17	+1.35	7.90	888	202		248		1.23
22			10/10	+1.50	8.95	954	174		129		0.74
23			10/29	+1.10	8.45	1023	191		70		0.37
24			10/30	+1.52	6.20	643	171		179		1.05
25	Homer City	4.0	10/15/69	+0.72	3.40	514	216		251		1.16
26			10/18	+1.40	12.15	1309	150		171		1.14
27			10/21	+0.28	12.30	1722		174	251	1.44	
28			10/24	+0.44	5.05	1067	262		246		0.94
29			4/21/70	+0.10	7.20	1655		120	186	1.55	
30			5/12	+0.60	9.70	1634	183		266		1.45
31			5/15	+1.13	10.5	1288	165		195		1.18
32			11/09	+0.60	16.75	2800	132		66		0.50
33	Keystone	4.8	10/23/67	+1.65	6.35	639	197		188		0.95
34			10/26	+0.17	10.10	1992		263	358	1.36	
35			10/28	+0.47	6.10	1240	237		179		0.76
36			10/29	+0.50	4.05	728	283		301		1.06
37		4.0	3/15/68	+0.30	11.70	2734	264		326		1.23
38			5/05	+0.31	7.05	1359	278		289		1.04
39			5/09	+1.15	12.55	1521	172		220		1.28
40			5/10	+0.72	5.25	803	266		256		0.96
41			5/11	+1.00	5.05	656	196		162		0.83
42			5/26	+1.90	6.85	646	172		124		0.72
43			10/20	+1.30	7.80	884	182		120		0.66
44			10/22	+1.80	6.10	588	150		153		1.02
45			10/26	+0.50	11.35	2047	238		291		1.22
46			10/30	+0.68	7.85	1211	248		241		0.97
47			10/31	+0.52	2.65	469	395		660		1.67
48			4/11/69	+0.09	4.05	1935		626	371	0.59	
49			4/28	+0.60	13.65	2316	208		123		0.59
50			10/09	+0.72	6.55	1004	182		256		1.41
51			10/31	+1.67	8.30	828	162		181		1.12
52			11/01	+0.30	11.70	2766	261		326		1.25
53	Homer City	4.0	10/11/69	+1.30	7.95	913	144		129		0.90
54			10/13	+0.95	9.00	1215	166		194		1.17
55			10/17	+0.20	13.90	1658		145	41	0.28	
56			10/20	+0.70	14.15	2210	151		126		0.83
57			11/06	-0.13	11.20	1545		162	169	1.04	
58			5/11/70	+0.52	5.15	929	266		267		1.00

Average values of $\frac{\text{observed plume rise}}{\text{calculated plume rise}}$

Neutral (11 cases) ~ 1.14

Stable (47 cases) ~ 1.03

X_{max} = downwind distance to maximum rise.

$s = \frac{g}{T}\frac{\partial\theta}{\partial z}$

g = gravity.

T = mean temperature in layer of plume rise.

F = buoyancy flux at stack top.

formula gives best predictions. Gross underpredictions occur mainly with neutral or unstable layers above a stable layer between stack top and plume centerline. The formula overpredicts rises in cases where a sharp inversion exists within or just above an otherwise neutral or slightly stable layer.

As indicated above, there were many instances when there existed considerable variability of the meteorological parameters within the plume-rise layer. For example, plumes frequently passed through shallow layers of differing vertical temperature gradients. This variability is certainly not unique to the Keystone-Homer City area — it is commonly observed with radiosonde observations over most of the globe. Because of such variability, one must expect substantial scatter in the ratio of observed to calculated plume rise in any set of field observations.

B. The Taylor Entrainment Hypothesis

For the special case of a buoyant plume in a crosswind, the Taylor entrainment assumption states that the rate at which ambient air enters the plume boundary is proportional to the characteristic velocity of the plume at any point, i.e., approximately, the wind speed. If R is a characteristic radius of the plume cross section, then by dimensional analysis,

$$R = \left(\frac{V}{U}\right)^{\frac{1}{2}}$$

where πV is the volume flux of the plume through a vertical plane. The entrainment assumption may thus be stated symbolically as

$$\frac{dV}{dz} = 2\gamma RU = 2\gamma (VU)^{\frac{1}{2}} \qquad (5)$$

where γ = a constant.

If U is assumed a constant, equation (5) may be integrated. At appreciable distances downwind it is permissable to treat the stack exit as a point source, and the resulting expression for the characteristic radius of the plume at any point during its rise is

$$R = \left(\frac{V}{U}\right)^{\frac{1}{2}} = \gamma z = \gamma \Delta h \qquad (6)$$

Briggs[5] suggests a value of 0.5 for the entrainment constant γ, based upon photographs of plumes at T.V.A. power plants.

Equation (6) is applicable to the "initial" phase of plume rise, where the entrainment is generated by the plume's upward motion (as discussed earlier, the later stage of rise is characterized by turbulent exchange between the plume and its environment). Briggs[5] has estimated $\gamma = 0.5$ from photographs of chimney plumes by relating plume radius to plume depth. In this study, the plume is observed far beyond this "initial" stage; and at this distance the observed distribution of SO_2 is near Gaussian, rather than forming a "top-hat" profile. Some questionable extrapolation is required in utilizing the LAPPES data to evaluate an "initial" phase entrainment constant (γ). However, such extrapolation is undertaken, since direct observational evidence of the entrainment rate is scarce, and possibly the LAPPES data can provide a numerical estimate of γ.

As noted, the Keystone and Homer City plumes attain full rise upwind from the cross-section measurements at 4 and 4.8 km. In order to arrive at an estimate of the entrainment constant, it is first necessary to adopt a procedure for estimating σ_{y_m} and σ_{z_m}, the cross-

wind and vertical-dimension parameters corresponding to the plume at X_{max}, the horizontal distance from the stack where maximum rise is attained. Values of X_{max} for each of the cases under study were listed in Table 6. If the plume cross sections are eliptical at this distance, then the characteristic radius may be defined as $2.15(\sigma_{y_m} \sigma_{z_m})^{\frac{1}{2}}$.

Turner[4] presents curves expressing the increase of σ_y and σ_z with downwind distance from the source for six categories of atmospheric stability. Based upon the discussion of the previous chapter, it appears that the 4 km values of σ_y and σ_z are generally underestimated by this model for elevated source applications. It is therefore inappropriate to expect realistic estimates of plume dimensions at X_{max} from the Turner curves unless suitable corrections for the observed discrepancies are employed. This can be accomplished by postulating virtual point sources upwind from the stacks. An example serves to illustrate this technique.

Suppose that according to Turner's σ_y curve for Class E stability a travel distance of 6 km is required to attain the value of σ_y measured at 4 km under moderately stable conditions. If the model employs a virtual point source 2 km upwind from the true source, then the value of σ_y read from the curve corresponds to the measured σ_y.

Further, assume that the distance downwind from the stack which corresponds to termination of plume rise is calculated from eq. (2) or eq. (4) to be 1.5 km. An estimate of σ_y at this point is obtained by following the curve back to the value which corresponds to 6-2.5=3.5 km. A similar correction may be applied to provide an estimate of σ_z at X_{max}. The virtual point source correction distances

need not be the same for σ_y and σ_z.

Using this technique, values of σ_{y_m} and σ_{z_m} were obtained for each of the LAPPES plumes measured at 4 and 4.8 km. The results are presented in Table 7. In the table corresponding values of mean wind speed and potential temperature gradient are also included. The virtual source correction distances, Δ_y and Δ_z, for adjusting σ_y and σ_z were determined from comparisons of observed 4-km plume dimensions with Turner's Class D values for neutral conditions, and Class E values for stable conditions. Negative values of Δ_y or Δ_z mean the measured value of σ_y or σ_z was actually less than the corresponding Turner value. For these cases, zero or unrealistically small values of σ_y or σ_z result from the extrapolation. Such cases are indicated by asterisks.

It is apparent from Figure 7 that there is an approximate linear relationship between plume rise and effective plume radius, as defined by $2.15(\sigma_{y_m} \sigma_{z_m})^{\frac{1}{2}}$. If a "top-hat" profile were assumed in a simulated plume, with an average concentration across this plume equal to the central concentration in the extrapolated Gaussian plume, the effective radius would be $\sqrt{2}(\sigma_{y_m} \sigma_{z_m})^{\frac{1}{2}}$. The slope of the line in Figure 7, i.e. the ratio of $2.15(\sigma_{y_m} \sigma_{z_m})^{\frac{1}{2}}$ to plume rise, is 1.3. Thus, with this definition of plume radius, $\gamma = 1.3$. For the simulated plume with a "top-hat" distribution, $\gamma = 0.85$.

Also, the average relationship between plume rise and the vertical depth may be computed. This is more directly analogous to Briggs' photographic comparisons between Δh and observed plume depth. For the extrapolated Gaussian plume, the half-depth is given by $2.15\sigma_{z_m}$;

Table 7

Relationahip Between Observed Plume Rise and Plume Radius at Distance of Maximum Rise

Case No.	Plant	Downwind Distance (km)	Date	$\partial\theta/\partial z$ $(\frac{^\circ C}{100m})$	$\bar{u}$ (mps)	Δ_y (km)	Δ_z (km)	σ_{y_m} (meters)	σ_{z_m} (meters)	plume radius $2.15(\sigma_{y_m}\sigma_{z_m})^{\frac{1}{2}}$ (meters)	observed plume rise (meters)
1	Keystone	4.8	10/21/67	+0.5	13.15	1.95	5.45	197	64	241	234
2			10/24	+1.7	7.13	4.3	1.4	225	34	188	203
3			10/27	+1.3	8.70	- 1.7	- 2.8	*	*	*	176
4			10/31	+2.7	6.10	2.7	- 2.6	197	*	*	122
5		4.0	3/18/68	+0.68	9.15	5.95	11.0	275	84	327	250
6			3/20	+0.10	9.50	- 0.80	- 1.4	66	*	*	218
7			4/01	+0.15	19.00	2.2	2.7	243	82	304	213
8			5/06	+0.85	6.95	11.0	2.6	483	47	324	199
9			5/07	+1.60	7.50	- 0.50	5.4	21	62	77	111
10			5/08	+0.90	10.25	2.8	0.2	191	28	158	120
11			5/09	+0.60	12.35	4.3	8.7	275	78	315	139
12			5/27	+0.20	12.70	- 0.2	2.75	108	84	205	150
13			7/04	+0.72	4.25	10.1	2.8	442	46	307	309
14			7/21	+0.73	2.65	39.0	6.5	1377	65	643	441
15			10/24	+0.70	5.45	5.9	22.2	290	116	395	420
16			4/09/69	+0.75	10.05	2.4	- 1.2	172	*	*	214
17			4/10	+0.24	12.65	0.85	1.1	178	64	229	260
18			4/14(1)	+1.80	4.15	12.8	1.2	528	28	264	134
19			4/14(2)	+0.22	2.85	7.5	0.6	540	60	387	646
20			4/15	+0.48	6.90	2.8	0.9	128	*	*	271
21			4/17	+1.35	7.90	6.1	13.0	301	93	360	248
22			10/10	+1.50	8.95	6.8	0.8	329	31	217	124
23			10/29	+1.10	8.45	6.6	- 2.6	322	*	*	70
24			10/30	+1.52	6.20	6.2	1.4	294	30	202	179
25	Homer City	4.0	10/15	+0.72	5.4	12.65	+ 0.9	526	26	251	251
26			10/18	+1.40	12.15	2.1	2.8	158	51	193	171
27			10/21	+0.28	12.3	1.3	2.1	190	75	256	251
28			10/24	+0.44	5.05	6.8	4.1	333	57	296	246
29			4/21/70	+0.10	16.75	0.85	- 1.6	160	15	105	186
30			5/12	+0.60	7.2	3.70	1.2	237	41	212	266
31			5/15	+1.13	9.7	10.3	14.0	470	97	459	145
32			11/09	+0.60	10.05	0.9	7.7	169	81	252	66
33	Keystone	4.8	10/23/67	+1.65	6.35	10.6	- 1.4	322	*	*	70
34			10/26	+0.17	10.10	- 1.6	- 0.2	*	47	*	358
35			10/28	+0.47	6.10	0.9	3.7	103	56	163	179
36			10/29	+0.50	4.05	2.4	1.8	144	38	159	301
37		4.0	3/15/68	+0.30	11.7	3.9	24.5	285	124	405	326
38			5/05	+0.31	7.05	11.9	32.0	529	137	578	289
39			5/09	+1.15	12.55	1.6	2.4	145	49	181	220
40			5/10	+0.72	5.25	0.05	6.5	47	68	122	256
41			5/11	+1.00	5.05	2.9	8.0	162	74	235	162
42			5/26	+1.90	6.85	4.6	1.6	234	36	197	124
43			10/20	+1.30	7.80	- 0.8	- 3.0	50	*	*	120
44			10/22	+1.80	6.10	4.9	5.7	241	63	265	153
45			10/26	+0.50	11.35	1.1	4.7	145	65	209	291
46			10/30	+0.68	7.85	2.5	- 0.4	170	18.5	121	241
47			10/31	+0.52	2.65	15.1	20.0	607	113	609	660
48			4/11/69	+0.09	4.05	3.2	10.6	309	155	470	371
49			4/28	+0.60	13.65	1.0	- 1.3	154	21.5	124	123
50			10/09	+0.72	6.55	9.0	4.5	414	56.5	329	256
51			10/31	+1.67	8.30	2.0	- 1.2	172	*	*	181
52			11/01	+0.30	11.70	4.8	2.6	322	58	284	326
53	Homer City	4.0	10/11/69	+1.30	7.95	4.2	- 0.1	227	*	*	129
54			10/13	+0.95	9.00	3.8	4.0	223	57	242	194
55			10/17	+0.20	13.90	1.8	- 2.0	217	*	*	41
56			10/20	+0.70	14.15	2.95	2.0	231	51	233	126
57			11/06	-0.13	11.20	3.2	3.8	284	91	347	169
58			5/11/70	+0.52	5.15	6.6	3.2	319	52	277	267

X_{max} = downwind distance to maximum plume rise.

σ_{y_m} = plume width parameter at X_{max}.

σ_{z_m} = plume depth parameter at X_{max}.

$2.15(\sigma_{y_m}\sigma_{z_m})^{\frac{1}{2}}$ = plume radius at X_{max}.

Δ_y, Δ_z = virtual source distances upwind from true source to achieve agreement with observed σ_y and σ_z at 4.0 or 4.8 km cross section using Turner's D and E curves.

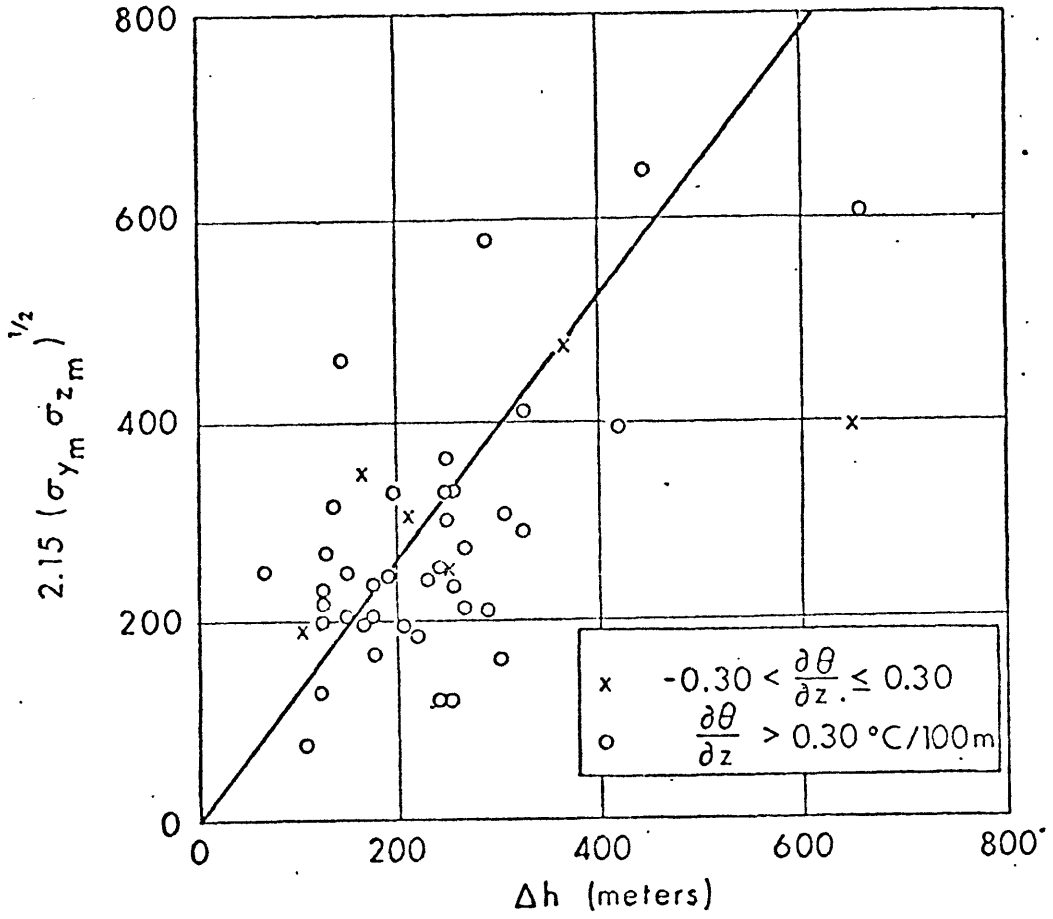

Figure 7

Keystone and Homer City Plants, Comparison of Observed Plume Rise, Δh with Cross Section Radius, $2.15(\sigma_{y_m} \sigma_{z_m})^{\frac{1}{2}}$

for the simulated "top-hat" plume, by $\sqrt{2}\,\sigma_{z_m}$. Based upon the average ratio $\sigma_{z_m}/\Delta h$ computed for the LAPPES cases, the entrainment constants for these definitions of plume radius are:

observed plume: $\gamma = 0.7$

simulated plume: $\gamma = 0.4$.

Better agreement with Briggs' value of 0.5 is seen when the plume radius is defined as the half-depth.

The anomalous cases in Table 7 mentioned above are characterized by unusually small 4-km values of σ_y or σ_z or both. Generally such cases occur under very stable conditions with at least moderately strong winds, or with neutral stability accompanied by very strong winds. These can hardly be considered determining criteria, however, since examples may be cited from Table 7 where similar atmospheric conditions failed to produce such small plume dimensions. As was observed in the previous chapter, the mean values of σ_y and σ_z measured at 4 km were considerably larger than those from Turner's curves. No satisfactory explanation is readily apparent for these few contrary cases.

Mean virtual point source correction distances, Δ_y and Δ_z, were computed for each of the six meteorological classifications defined earlier in Table 5. In Table 8 the results are presented. In calculating mean values of Δ_y and Δ_z, the highest and lowest individual values in each category were discarded to prevent distortion by unrepresentative extremes. The use of Table 8 is recommended for elevated-source applications under near-neutral and stable conditions. The corrections apply to Turner's stability categories D and E respectively. The values of Δ_y and Δ_z are to be added to the downwind distance at

Table 8

Mean Virtual Source Correction Distances Necessary To Achieve Agreement with Measured σ_y and σ_z Values Using Turner's Curves for Stability Categories D and E

Class No.	Range of $\partial\theta/\partial z$ (°C/100m)	Windspeed	Δ_y (km)	Turner Stability Category	Δ_z (km)
1	$-0.3 < \frac{\partial\theta}{\partial z} < 0.3$	$\bar{U} > 8$ mps	1.6	D	2.1
2	$-0.3 < \frac{\partial\theta}{\partial z} < 0.3$	$\bar{U} < 8$ mps	5.3*	D	5.6*
3	$0.3 \geq \frac{\partial\theta}{\partial z} < 1.0$	$\bar{U} > 8$ mps	3.0	E	5.1
4	$0.3 \geq \frac{\partial\theta}{\partial z} < 1.0$	$\bar{U} < 8$ mps	7.2	E	5.7
5	$\partial\theta/\partial z \geq 1.0$	$\bar{U} > 8$ mps	4.4	E	2.0
6	$\partial\theta/\partial z \geq 1.0$	$\bar{U} < 8$ mps	4.8	E	3.9

*Averages based on only two cases.

which concentrations are to be computed with the Turner model.

C. Correlations Between Plume Dimensions and Meteorological Variables at the Downwind Distance of Maximum Plume Rise

For hot effluents released from large industrial stacks, the rate of mixing with ambient air is initially governed by the original properties of the plume gases themselves and by the environmental vertical temperature structure, horizontal momentum, and directional wind shear. At some point, downwind, however, ambient turbulence begins to exert a major influence on the entrainment process. Briggs[12] has suggested that this distance may be estimated by $X^* = 0.285X_{max}$. The mixing which takes place in the interval between X^* and X_{max} is presumably similar to the turbulent diffusion which occurs after the plume attains its full rise, the main difference being in the sizes of the eddies which dominate the mixing in the two regimes.

It is of interest to determine whether relationships between plume dimensions at X_{max} and the meteorological variables are appreciably different from those observed at 4 km (see Chapter IV). At issue here is the question of whether the influence of the initial conditions continues to be significant as the plume completes its rise. In Table 9 the correlation coefficients obtained at 4 km are compared with those corresponding to the distance of maximum plume rise. From inspection of the table it is obvious that the two sets of statistics are nearly identical. Similarity was to be anticipated, however, due to the technique by which σ_{y_m} and σ_{z_m} were determined (see V-B), and because nearly all of the cases available correspond to stable conditions, when the effect of ambient turbulence is smallest. This is simply a

statement of a major hypothesis of the present investigation: in a stable atmosphere, entrainment, i.e. the mixing with environmental air which occurs in a rising plume, effectively determines the relative size and shape of the plume at distances well beyond the point where eddies become important. The plume at 4 km equals the plume at X_{max} plus the growth due to diffusion in the interval between. Diffusion for the stable cases proceeds slowly. It is the entrainment during plume rise which leads to the large values of σ_y and σ_z observed at 4 km and which invalidates the use of a virtual point source directly above the stack for large stack applications.

Table 9

Correlations between Plume Size-Shape Parameters and Meteorological Parameters at 4 km and at X_{max}

Variables		Correlation Coefficients	
X	Y	X_{max}	4 km
$\bar{U}$	σ_y	-0.44	-0.51
A	σ_y	0.65	0.68
$\partial\theta/\partial z$	σ_y	-0.05	-0.05
$\bar{U}$	σ_z	0.01	-0.03
A	σ_z	-0.19	-0.08
$\partial\theta/\partial z$	σ_z	-0.48	-0.54
$\bar{U}$	$\sigma_y\sigma_z$	-0.29	-0.47
A	$\sigma_y\sigma_z$	0.43	0.42
$\partial\theta/\partial z$	$\sigma_y\sigma_z$	-0.26	-0.34
$\bar{U}$	σ_z/σ_y	.06	0.36
A	σ_z/σ_y	-0.35	-0.29
$\partial\theta/\partial z$	σ_z/σ_y	0.08	-0.57

VI. CONCLUSIONS AND RECOMMENDATIONS

Evidence presented in this paper suggests that commonly-employed diffusion models are inadequate to describe the diffusion of an effluent emitted from a tall stack. Specifically, it has been demonstrated that models which employ Turner's diffusion coefficients generally underestimate the rate of plume growth at heights of several hundred meters above the ground. The obvious deduction to be made from this observation is that such models must overestimate ground-level concentrations associated with elevated emissions for neutral and stable conditions. Unfortunately, no data corresponding to unstable conditions with light winds were available. It would be of particular interest to determine whether similar discrepancies exist for such situations, since these conditions are normally associated with maximum ground-level concentrations from elevated sources.

(1) The virtual source correction distances proposed in Chapter V may be conveniently used with Turner's coefficients, σ_y and σ_z, to improve predictions of concentrations for tall-stack applications. The LAPPES plume data measurements corresponded to stable and neutral conditions. Correction distances for unstable conditions could be similarly derived should appropriate data become available. It is important to view the virtual source technique as merely a useful interim tool to improve the quality of diffusion modelling for a specific type of application. Such a technique does little to enhance understanding of the actual physics of plume spread. A definitive treatment awaits a systematic study of the relationships between turbulent structure and plume characteristics at higher levels.

(2) The strong relationships between plume size and both wind speed and the vertical variability of the wind are clearly established by this study. With very light winds, plume rise is highest. Both the inherent variability of the wind direction with low winds, and the fact that the plume passes through a deeper atmospheric layer mitigate in favor of large, diffuse cross sections. The traditional assumption of an inverse proportionality between wind speed and downwind concentration ignores the correlation between wind speed and directional shear, and may be expected to break down in the case of light winds.

(3) If the total rise of the plume is simulated by the Taylor entrainment process for the "initial stage" of the rise, one arrives at entrainment constants whose magnitudes depend on the definition of the "edge of the plume". A value similar to Briggs' is obtained when the characteristic plume radius is taken to be the half-depth.

(4) Under the meteorological conditions prevailing during the LAPPES experiments, it appears that entrainment in a rising plume produces cross sections of considerably larger sizes than can be explained by eddy diffusion from a point source. For stable air, the initial stages of entrainment effectively determine the relative size and shape of plume cross sections at least as far as downwind from the source as 4 km. More data corresponding to neutral and unstable cases is needed to evaluate the importance of the initial entrainment processes under these conditions.

APPENDIX I

In Chapter II, a crude mass balance calculation was employed for the purpose of selecting reliable plume cross-section measurements. A ratio of the SO_2 flux through the cross sections to the known emission rate was computed for each measurement made at 4 and 4.8 km. In only about half of the available cases was the requirement of 50% mass balance satisfied. Some of the mass loss is undoubtedly attributable to limitations inherent in the experimental techniques employed in the LAPPES experiments. However, in view of several recent studies concerned with the oxidation of SO_2 in the atmosphere, it seems reasonable that chemical decay may also be a factor worthy of some consideration.

A thorough treatment of this form of plume attenuation is outside the scope of the present investigation. However, the LAPPES data does contain information which may be of value to the reader interested in chemical conversion processes. Hence, for completeness, a brief summary of the relevant data is presented below.

Investigations into the importance of SO_2 oxidation usually adopt an approach based on simultaneous measurements of SO_2 and some relatively inert tracer material. Assuming that both substances are similarly acted upon by diffusive mechanisms in the atmosphere, it is theoretically possible to attribute differences in the ratio of their respective concentrations at successive downwind distances to the chemical conversion of SO_2.

Several measurement techniques and a variety of tracers have been employed in efforts to quantitatively describe this effect. Weber[11]

analyzed simultaneous ground-level concentrations of SO_2 and CO_2 at a point downwind from a power plant in Germany. His results indicate that the half-life of SO_2 in stack plumes may be of the order of 20 minutes to an hour in a neutral or stable atmosphere. Dennis, et al[13], arrived at a similar value, using another experimental technique. Stephens and McCaldin[14] traversed SO_2 plumes in an instrumented aircraft and found a strong correlation between oxidation rate and relative humidity. In this case submicron particulate matter was the designated tracer. Some doubt exists as to the validity of this apparent humidity dependence, since the light-scattering particle counter employed in the experiments has been shown to be influenced by humidity. Efforts by Gartrell, et al[15], to associate humidity with SO_2 decay rate also produced somewhat ambiguous results. A large-scale pollutant transport model used by J. Nordö[16], Norwegian Meteorological Institute, assumes a decay rate proportional to the concentration in the plume. The half-life corresponding to an SO_2 concentration of $1 mg/m^3$ is about 1/2 hour.

The analysis of the LAPPES data in this context must be attempted without benefit of tracer comparisons. However, wind and humidity data corresponding to many of the cross-section measurements are available. The residence time of the SO_2 in a given plume cross section at 4 km can be inferred from the mean wind speed as determined by the concurrent pilot balloon ascent. Helicopter measurements provide values of wet-bulb and dry-bulb temperatures at the stack exit height, and the relative humidity thus determined from tables.

The data for 61 4-km cross sections were grouped into 9 categories

corresponding to various ranges of mean wind speed and relative humidity at stack height. In Table 10 the mean values of the ratio of the cross-sectional SO_2 mass flux to emission rate for each category are presented. A positive relationship between SO_2 oxidation and relative humidity would manifest itself in the table by larger ratios in the top boxes. Such a correlation is not seen with the LAPPES data. Similar ambiguity exists in comparing the rates corresponding to various atmospheric residence times, although there appears to be some tendency toward higher mass balance ratios with strong winds.

The LAPPES data afford little insight into non-diffusive SO_2 removal processes. Certainly, experiments using tracer substances are more appropriate for a study of these processes. The importance of considering SO_2 decay rate in this investigation is chiefly a matter of establishing the credibility of the plume cross-section measurements analyzed in the previous chapters of this paper. The evidence presented in the studies cited above demonstrates that chemical removal processes do attenuate SO_2 plumes to an extent which should appreciably affect the mass balance calculations made for the purposes of this investigation. Thus, the relatively low percentage of emitted SO_2 found in the 4-km cross-sections need not reflect unfavorably on the quality of the measurement techniques employed in the LAPPES data.

Table 10

Ratios of 4 km Cross-Sectional SO_2

Mass Flux to Stack Emission Rate for 9 Categories of
Wind Speed and Relative Humidity at Stack Exit Height

	$\bar{U} \leq 5$ mps	5 mps $< \bar{U} \leq 10$ mps	$\bar{U} > 10$ mps	weighted means ↓
RH ≤ 63%	0.46 (6 cases)	0.59 (9 cases)	0.52 (6 cases)	0.53
65% < RH ≤ 80%	0.31 (5 cases)	0.44 (9 cases)	0.60 (10 cases)	0.48
RH > 80%	0.50 (3 cases)	0.70 (8 cases)	0.53 (5 cases)	0.61
weighted means →	0.41	0.57	0.56	

REFERENCES

1. Pasquill, F., 1961: The estimation of the dispersion of windborne material. Meteorol. Mag., 90, 1063, pp 33-49.

2. Cramer, H. E., 1957: A practical method for estimating the dispersion of atmospheric contaminants. Proc. 1st Natl. Conf. on Appl. Meteorol., Amer. Meteorol. Soc.

3. Gifford, F. A., 1961: Uses of routine meteorological observations for estimating atmospheric dispersion. Nuclear Safety, 2,4, pp 47-51.

4. Turner, D. B., "Workbook of Atmospheric Dispersion Estimates", U. S. Department of Health, Education and Welfare, National Air Pollution Control Association, Cincinnati, Ohio (Revised 1969).

5. Briggs, G. A., 1969: "Plume Rise", AEC Critical Review Series.

6. Slawson, P. R. and G. T. Csanady, 1971: The effect of atmospheric conditions on plume rise. J. Fluid Mech., 47, part 1, pp 33-49.

7. Taylor, G. I., 1945: Dynamics of a mass of hot gas rising in the air, USAEC Report MDDC-919 (LADC-276), Los Alamos Scientific Laboratory.

8. Halitsky, J., C. P. Randell, and M. Hackman, 1950: Communications on Dust Deposition from Chimney Stacks. Discussion by C. H. Bosanquet, et al, Proc. Inst. Mech. Eng., Nos. 1-4, p 366.

9. Priestley, C. B. H., 1956: A working theory of the bent-over plume of hot gas, Quart. J. Roy. Meteorol. Soc., 82, pp 165-176.

10. Schiermeir, Francis A., 1970: "Large Power Plant Effluent Study." Instrumentation, Procedures, and Data Tabulations. U. S. Department of Health, Education and Welfare, Public Health Service, Environmental Health Service (3 vols).

11. Weber, Erich, 1970: Contribution to the residence time of SO_2 in a polluted atmosphere. J. Geoph. Res., Vol 75, No. 15, pp 2902-2914.

12. Briggs, G. A., 1970: Recent Analysis of Plume Rise Observations. Paper presented at the 1970 International Air Pollution Conference.

13. Dennis, R., C. E. Billings, F. A. Record, P. Warneck, and M. L. Arin, 1969: "Measurements of Sulfur Dioxide Losses from Stack Plumes", APCA Paper No. 69-156, 62nd Annual Meeting of the Air Pollution Control Association, New York City, June 26, 1969.

14. Stephens, N. Thomas, and Roy O. McCaldin, 1971: Attenuation of power station plumes as determined by instrumented aircraft. Environmental Science and Technology, 5, pp 615-621.

15. Gartrell, F. E., F. W. Thomas, and F. W. Carpenter, 1964: "Full-Scale Study of Dispersion of Stack Gases", a summary report by Tennessee Valley Authority and U. S. Public Health Service, Chatanooga, Tennessee, August, 1964.

16. Nordö, J.: Norwegian Meteorological Institute, personal communication.